



Novel Materials for High Coherence Superconducting Quantum Devices

Mustafa Bal

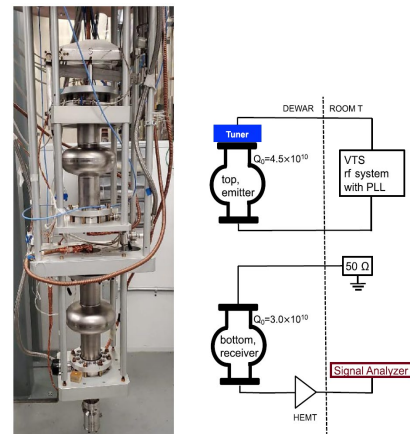
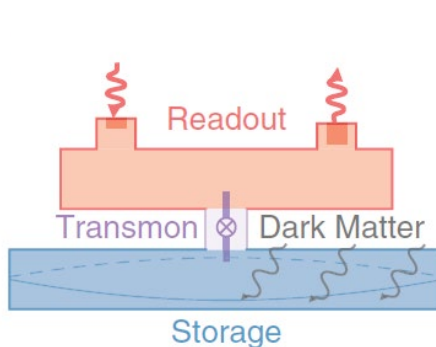
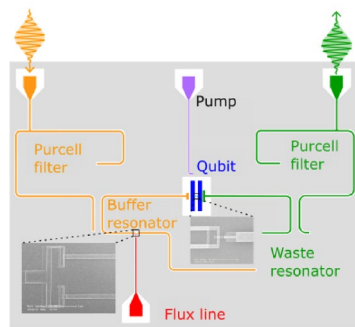
SQMS Qubit Fabrication Group Leader



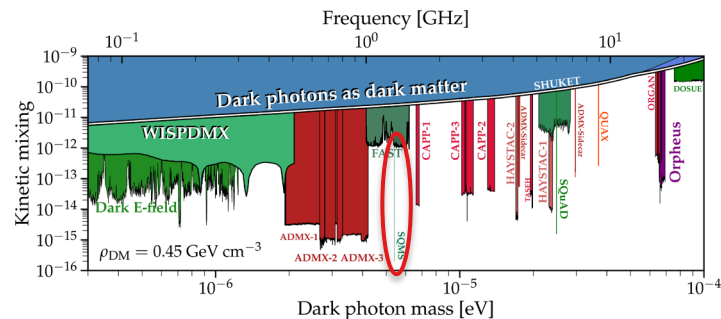
This manuscript has been authored by Fermi Research Alliance, LLC under Contract No. DE-AC02-07CH11359 with the U.S. Department of Energy, Office of Science, Office of High Energy Physics.

Superconducting Devices for Dark Matter Experiments

- SRF Cavities
- Qubits
- JJ based Single Photon Counters
- Quantum Limited Amplifiers
- Microwave Kinetic Inductance Detectors (MKIDs)
- Transition Edge Sensors
-

A. Romanenko et al, PRL **130**, 261801 (2023)A. V. Dixit et al, PRL **126**, 141302 (2021)

L. Balembois et al, arXiv:2307.03614 (2023)



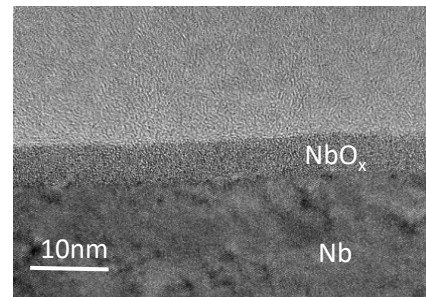
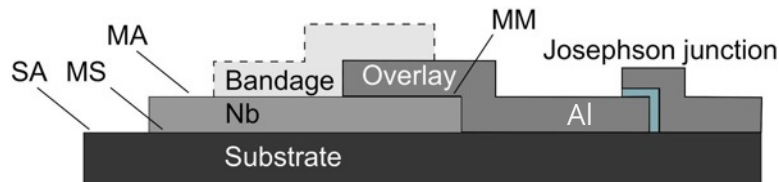
R. Cervantes et al, arXiv:2208.03183 (2022)

Decoherence channels in 2D superconducting qubits: two-level systems, bulk substrate losses, quasiparticles, ...

$$\gamma = \sum_i \gamma_i + \Gamma = \omega \sum_i p_i \tan \delta_i + \Gamma$$

Total decay rate ^{1,2,3} $\rightarrow \gamma$
 Other channels (e.g. radiative decay) $\rightarrow \Gamma$
 Participation ratio $E_{\text{stored}}/E_{\text{total}}$ $\rightarrow p_i$
 Lossy elements with known $E_{\text{stored}}/E_{\text{total}}$ $\rightarrow \gamma_i$
 Qubit frequency $\rightarrow \omega$
 Loss tangent $\rightarrow \tan \delta_i$

MS: Metal-Substrate | SA: Substrate-Air | MA: Metal-Air | MM: Metal-Metal



Each channel bounds T_1 :

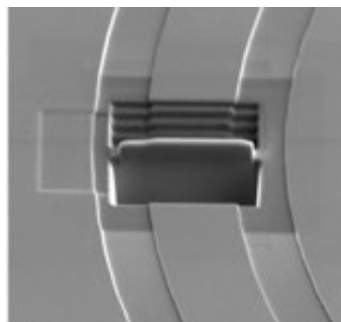
Looking for changes channel-by-channel:

$$T_1 \leq 1/\gamma_i \quad \Delta\gamma = \sum_i \delta\gamma_i$$

1. Koch, J. *et al.* Physical Review A **76**, 042319 (2007)
2. Wenner, J. *et al.* Applied Physics Letters **99**, 113513 (2011)
3. Wang *et al.* Appl. Phys. Lett. **107**, 162601 (2015)
4. Calusine, G. *et al.* Applied Physics Letters **112**, 062601 (2018)

SQMS innovative approaches quantum materials and devices characterization

Dissecting and studying fragments of characterized devices



rigetti

Cryogenic TEM, AFM, MFM

Cryo XRD, XRR

Cryogenic TOF-SIMS

Atom Probe Tomography

THz spectroscopy

Magneto Optical Imaging

β -NMR, μ SR



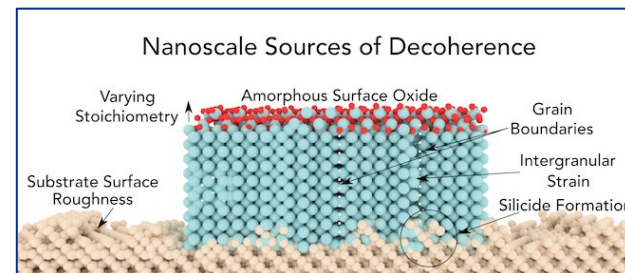
Northwestern
University

NUANCE
Northwestern University Atomic and
Nanoscale Characterization Experimental Center



SIF SENSITIVE
INSTRUMENT
FACILITY

Fermilab



A. A. Murthy et al, ACS Nano **16**, 17257 (2022)



**SUPERCONDUCTING QUANTUM
MATERIALS & SYSTEMS CENTER**

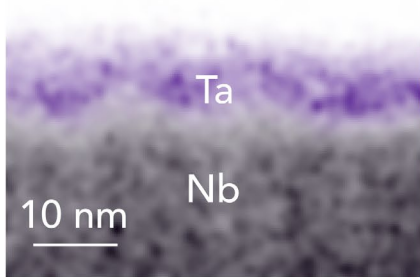
- Leveraging DOE and SQMS academic partners user facilities capabilities to identify sources of decoherence

Novel Surface Encapsulation as Mitigation Strategy to eliminate Nb_2O_5

- Avoid niobium oxidation by stable surface **encapsulating layer**
 - Thin ($\sim 5\text{-}10\text{ nm}$) => small contribution to conductive losses
 - But TLS-hosting dissipative surface Nb_2O_5 is absent => reduction of the TLS dielectric losses => better coherence

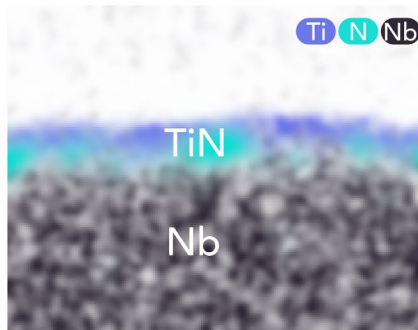
Ta Encapsulation

Ta Nb



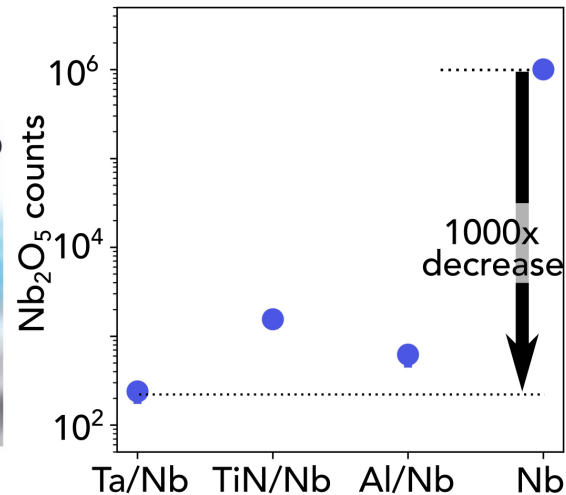
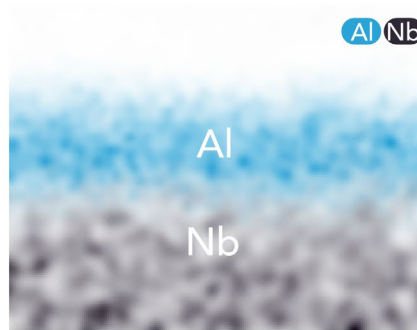
TiN Encapsulation

Ti N Nb

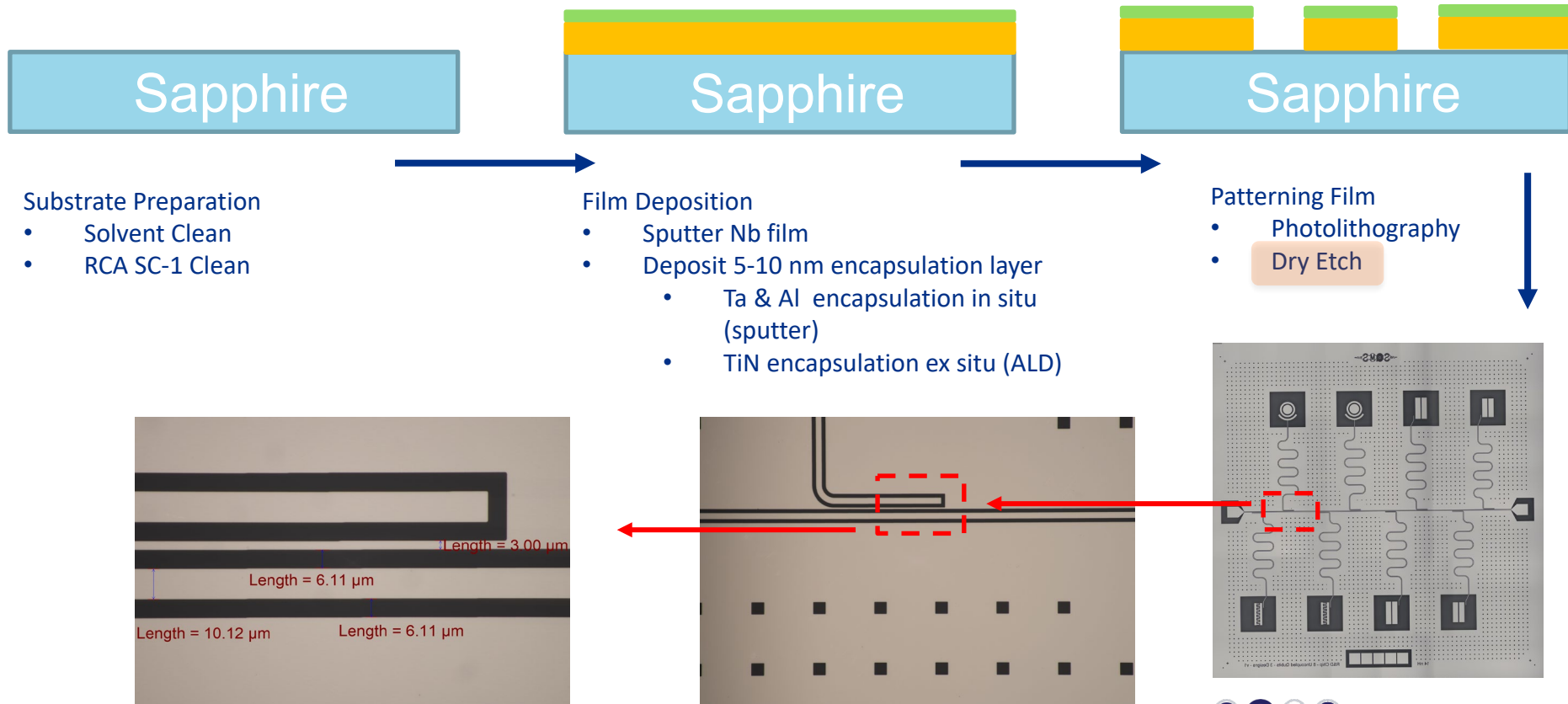


Al Encapsulation

Al Nb

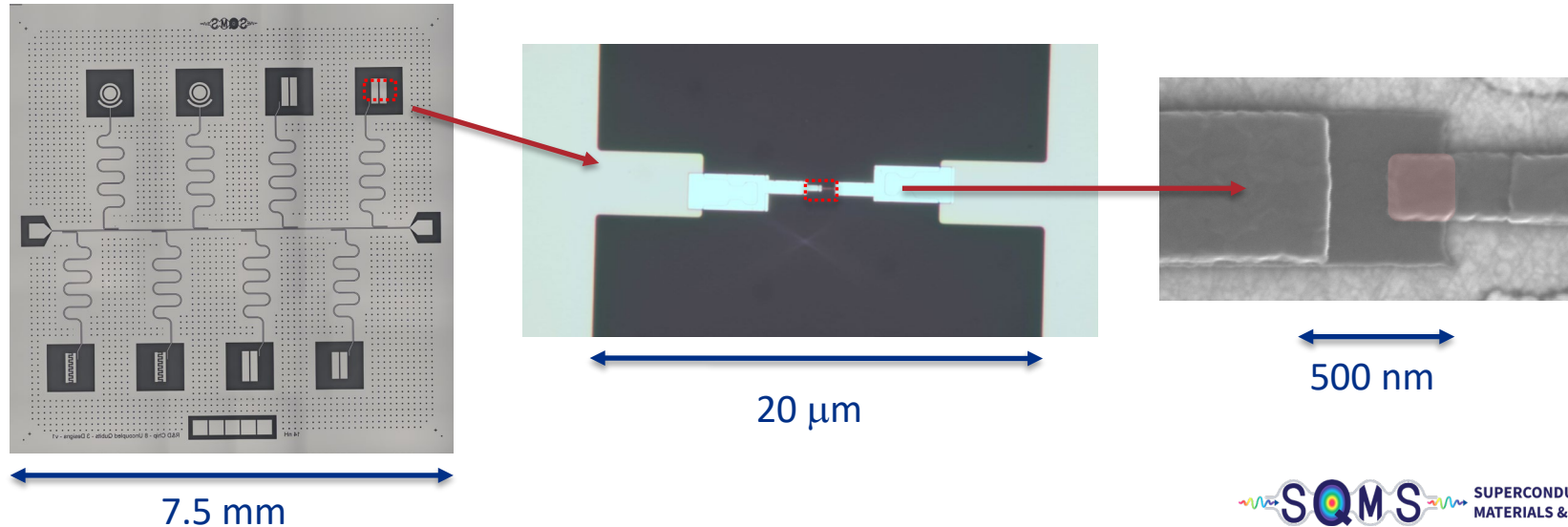


Process Flow to Define Qubit Circuitry on Sapphire

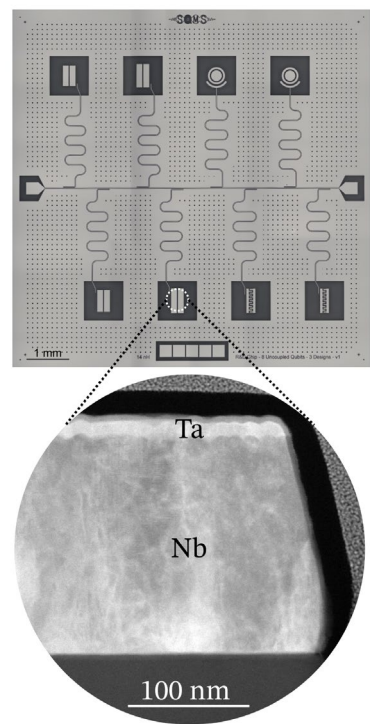


Josephson Junction Fabrication

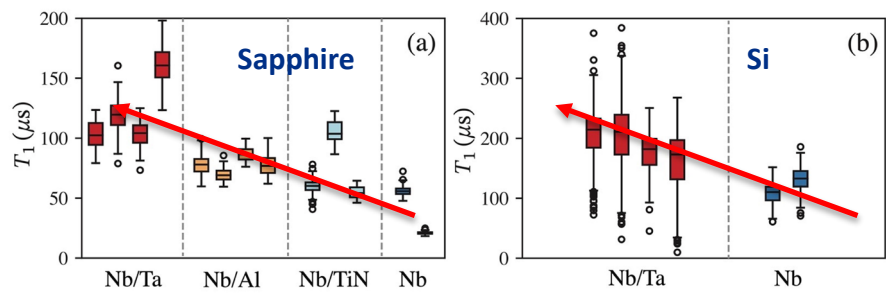
- Al/AlOx/Al Junctions are deposited at +22 / -22 degree angles relative to the normal of the substrate.
- 2'15" (45"/45"/45" at +60/0/-60 degree) Ar ion milling to remove oxide on Nb.
- Bottom/Top electrode thicknesses are 40 nm/90 nm.
- The Oxidation is 20 mBar for 12 minutes (Ar/O₂ (85/15) mixture)
- Typical Junction area is approximately 200 nm x 200 nm



Qubit Coherence Results



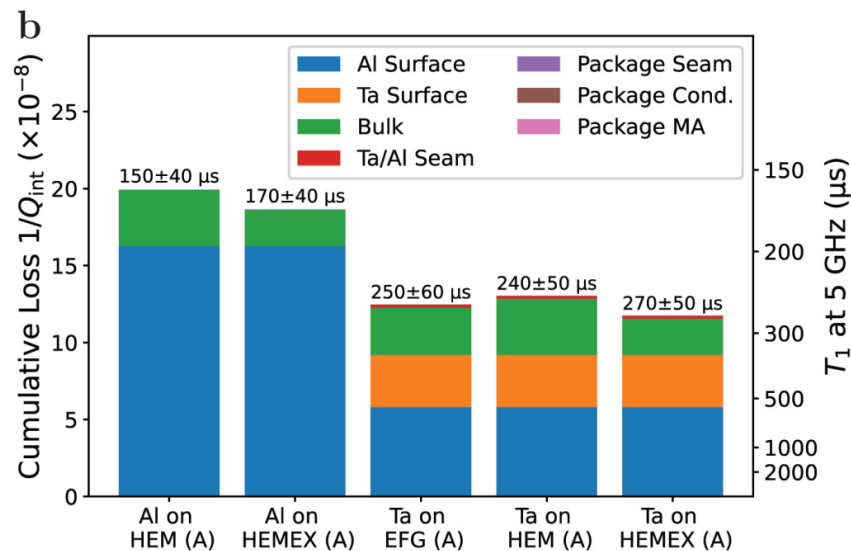
M. Bal et al, arXiv:2304.13257 (2023)



Group	Best T_1 (μ s)	Freq. (GHz)	Substrate	Primary Material	Publication Year
Yu	503	3.8-4.7	Sapphire	Ta, dry etch	2022
SQMS	451	4.5-5	Silicon	Ta/Nb, dry etch	2023
Houck	360	3.1-5.5	Sapphire	Ta, wet etch	2021
IBM	340	~4	Silicon	Nb, dry etch	2022
IBM	234	3.808	Silicon	Al, dry etch	2021
SQMS	198	4.5-5	Sapphire	Ta/Nb, dry etch	2023

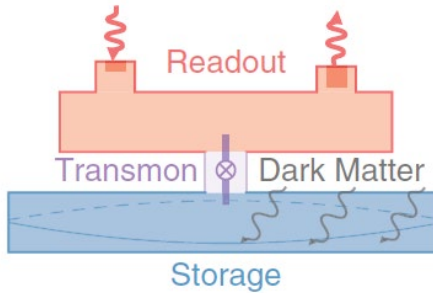
Elimination of Surface Losses Critical for T_1 beyond ms time scales

- Explore novel surface encapsulations (Au, PdAu, NbN,...)
 - Nb/Au – 181 +/- 15 μs
- Different SC materials (Ta, TiN, NbTiN,...)
- Reduce bulk dielectric losses (Annealing, impurities,...)

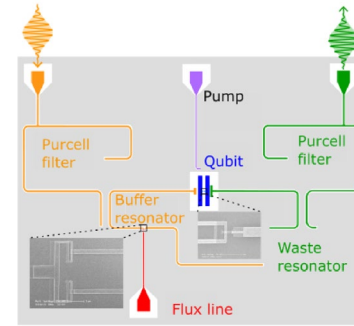


S. Ganjam et al, arXiv:2308.15539 (2023)

Qubits for Dark Matter Search



A. V. Dixit et al, PRL **126**, 141302 (2021)



L. Balembouis et al, arXiv:2307.03614 (2023)

Experiments to use these devices for Axion search.

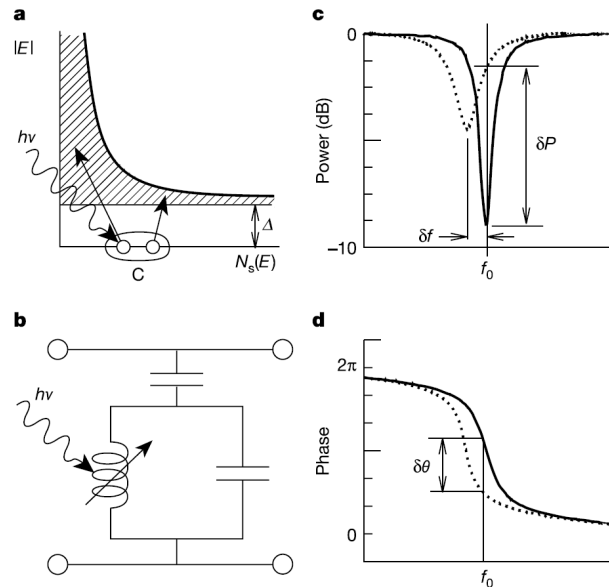
MKIDs

Applications include:

- Observational Astronomy
- Dark Matter Search
- Neutrino Detection
- QIS

Noise Sources:

- TLS noise
- Shot noise from the generation and recombination of quasiparticles
- Amplifier noise



P. K. Day et al, Nature **425**, 817 (2003)

Acknowledgments



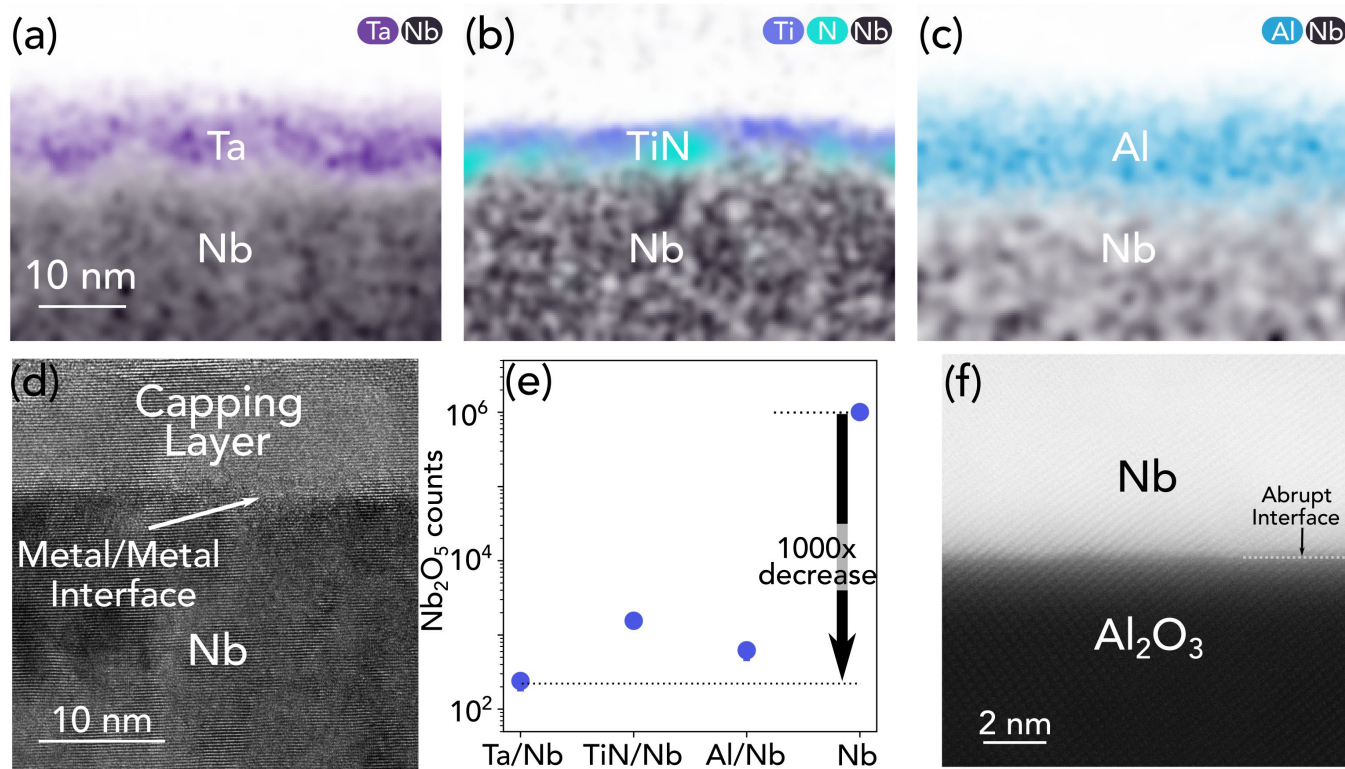
Akshay A. Murthy
Francesco Crisa
Sabrina Garattoni
Shaojiang Zhu
Xinyuan You
Ziwen Huang
ZuHawn Sung
Jaeyel Lee
Daniel Bafia
David van Zanten
Ivan Nekrashevich
Tanay Roy
Yulia Krasnikova
Roman Pilipenko
Alexander Romanenko
Anna Grassellino

Cameron J. Kopas
Ella O. Lachman
Duncan Miller
Josh Y. Mutus
Matthew J. Reagor
Hilal Cansizoglu
Jayss Marshall
David P. Pappas

Florent Q. Lecocq
Michael R. Vissers
David Olaya
Jose Aumentado
Joel N. Ullom
Peter Hopkins

Dominic P. Goronzy
Carlos G. Torres-Castanedo
Graham Pritchard
Vinayak P. Dravid
James M. Rondinelli
Michael J. Bedzyk
Mark C. Hersam
Jens Koch

Effectiveness of Passivation



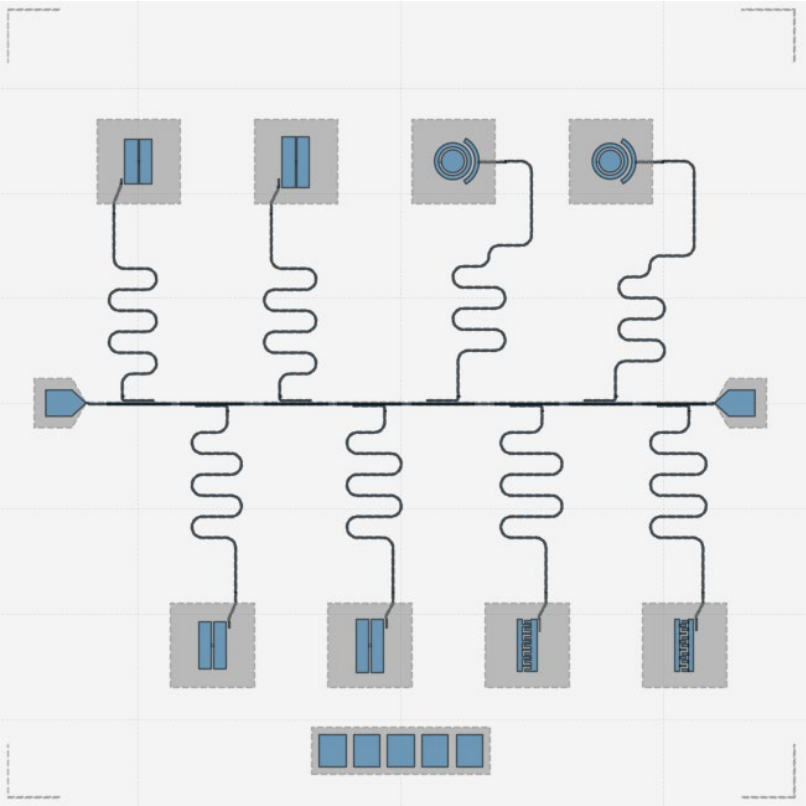
Design parameters and device layout

14pH, Sapphire=10.0

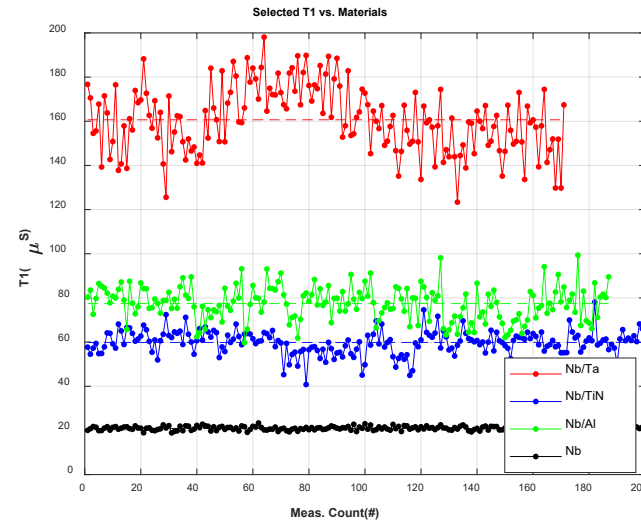
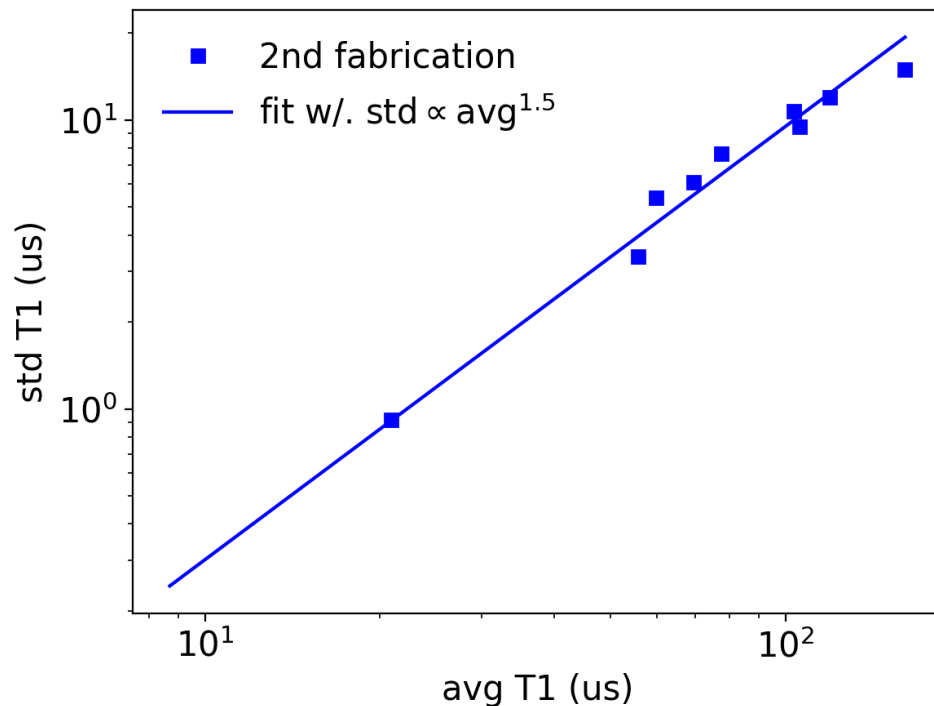
	L	f_r	f_{01}	χ	α	g	κ	Q_c	γ
0	4047.0	7505.0	5055.0	0.46	308.0	88.0	0.75	10000	0.0010
1	4151.0	7327.0	4914.0	0.47	290.0	91.0	0.73	10000	0.0010
2	4260.0	7147.0	4784.0	0.49	274.0	94.0	0.71	10000	0.0011
3	4376.0	6965.0	4663.0	0.50	259.0	95.0	0.70	10000	0.0012

	L	f_r	f_{01}	χ	α	g	κ	Q_c	γ
0	4497.0	6760.0	4526.0	0.5	242.0	96.0	0.68	10000	0.0012
1	4626.0	6571.0	4410.0	0.5	229.0	95.0	0.66	10000	0.0013

	L	f_r	f_{01}	χ	α	g	κ	Q_c	γ
0	4762.0	6093.0	4364.0	0.66	225.0	88.0	0.61	10000	0.0016
1	4906.0	5934.0	4250.0	0.50	213.0	76.0	0.59	10000	0.0012



T1 variation due to TLS



Average T1 vs. Standard variation T1

$$\langle T_1 \rangle = \frac{1}{\kappa^2 N M^2 \omega \pi} \quad \sigma_{T_1} = \frac{G}{2\gamma_{\phi}^{\frac{3}{2}} \kappa^2 N^{\frac{3}{2}} M^2 \omega^{\frac{3}{2}} \pi^{\frac{3}{2}}}$$

Assume variation due to number of TLS

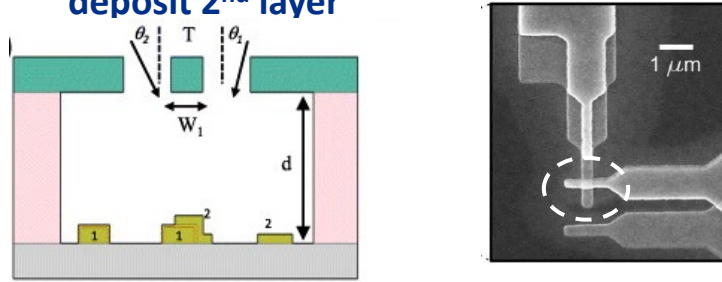
$$\sigma_{T_1} \propto \langle T_1 \rangle^{3/2}$$

X. You, et al., Phys. Rev. Appl. **18**, 044026 (2022)

Liftoff Process to Fabricate Submicron Al/AlOx/Al Junctions

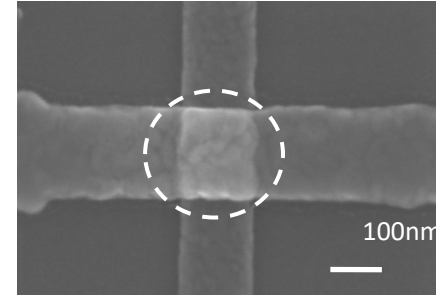
Shadow evaporation with tilt, “Dolan bridge” –
Single pattern step, single pumpdown

- 1) Pattern, deposit 1st layer, oxidize, tilt,
deposit 2nd layer



Overlap junction - 2 patterns, pumpdowns

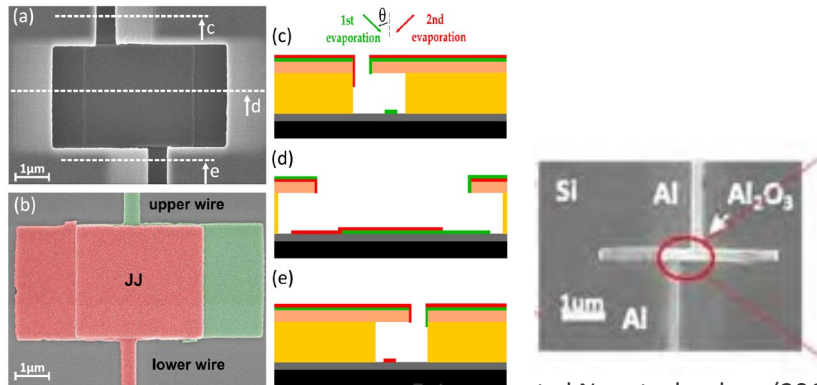
- 1) Pattern
pumpdown
LO BE
- 2) Pattern
pump down
mill BE & oxidize
LO TE



X. Wu, et. al APL (2017)

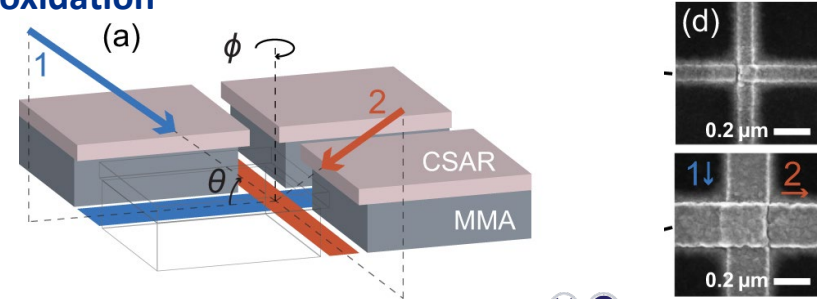
M. Steffen et. al, PRL97, 050502 (2006)

“Bridgeless” – shadow evaporation in high aspect tilt



F. Lecocq et al Nanotechnology (2011)

“Manhattan style” – shadow evaporation
Use rotation between the two depositions and oxidation

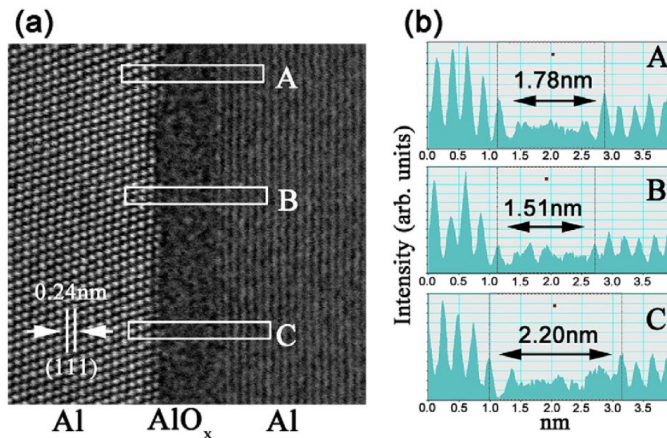
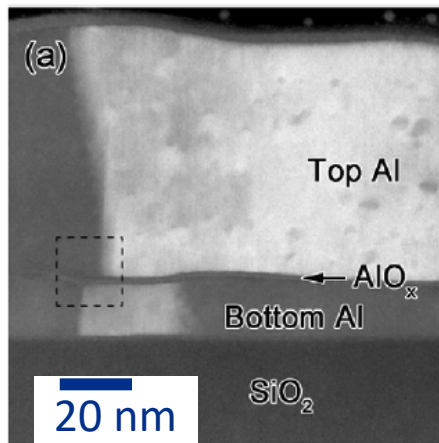


J M Kreikebaum et al 2020 Supercond. Sci. Technol. 33 06LT02

Josephson junctions - sensitive to atomic-level defects

- Aluminum oxidation is conformal, ~ 1.8 nm thick Al/AlO_x/Al
- Thickness variations with exponential dependence of current
 - Less than 10% of total barrier active
 - Strong inhomogeneity of tunnel current across junction
- Amorphous materials are lossy – make junctions small

Cross-section TEM



Zeng, J. Phys. D: Appl. Phys. **48** (2015) 395308

Dolan Bridge Double Angle Shadow Evaporation



Raith EBPG5200 E-Beam lithography system (100 kV)

t1: thickness of 1st resist layer
t2: thickness of 2nd resist layer
m1: 1st metal deposition thickness
m2: 2nd metal deposition thickness
 θ_1 : 1st deposition angle
 θ_2 : 2nd deposition angle
b: bridge width

